

COEFF-KANS: A Paradigm to Address the Electrolyte Field with KANS

Xinhe Li^{1,3*}, Zhuoying Feng^{1,3*}, Yezeng Chen^{2,3*}, Weichen Dai^{1,3}, Zixu He¹,
Yi Zhou^{1,3†}, Shuhong Jiao^{1†}

¹University of Science and Technology of China

²ShanghaiTech University

³Knowledge Computing Lab

lixinhe669@gmail.com, zoeyfeng@mail.ustc.edu.cn, chenyz2022@shanghaitech.edu.cn, dddwc@mail.ustc.edu.cn,
hzx123@mail.ustc.edu.cn, yi_zhou@ustc.edu.cn, jiaosh@ustc.edu.cn

Abstract

To reduce the experimental validation workload for chemical researchers and accelerate the design and optimization of high-energy-density lithium metal batteries, we aim to leverage models to automatically predict Coulombic Efficiency (CE) based on the composition of liquid electrolytes. There are mainly two representative paradigms in existing methods: machine learning and deep learning. However, the former requires intelligent input feature selection and reliable computational methods, leading to error propagation from feature estimation to model prediction, while the latter (e.g. MultiModal-MoLFormer) faces challenges of poor predictive performance and overfitting due to limited diversity in augmented data. To tackle these issues, we propose a novel method COEFF (COLUMbic Efficiency prediction via Fine-tuned models), which consists of two stages: pre-training a chemical general model and fine-tuning on downstream domain data. Firstly, we adopt the publicly available MoLFormer model to obtain feature vectors for each solvent and salt in the electrolyte. Then, we perform a weighted average of embeddings for each token across all molecules, with weights determined by the respective electrolyte component ratios. Finally, we input the obtained electrolyte features into a Multi-layer Perceptron or Kolmogorov-Arnold Network to predict CE. Experimental results on a real-world dataset demonstrate that our method achieves SOTA for predicting CE compared to all baselines. Data and code used in this work will be made publicly available after the paper is published.

Introduction

The discovery and optimization of battery electrolytes are crucial in climate and sustainable technology due to their potential to accelerate decarbonization in all economic sectors (Agre, Molina, and Chu 2017; Tian et al. 2020). Enhancing Coulombic Efficiency (CE) is vital for the adoption of high-energy-density lithium metal batteries (Liu et al. 2023a; Yuan et al. 2021). Liquid electrolyte engineering is a promising strategy for improving CE, but its complexity makes it challenging to predict and design electrolyte performance (Aykol, Herring, and Anapolsky 2020). For example, high-throughput screening accelerates the search

*These authors contributed equally.

†Corresponding Authors.

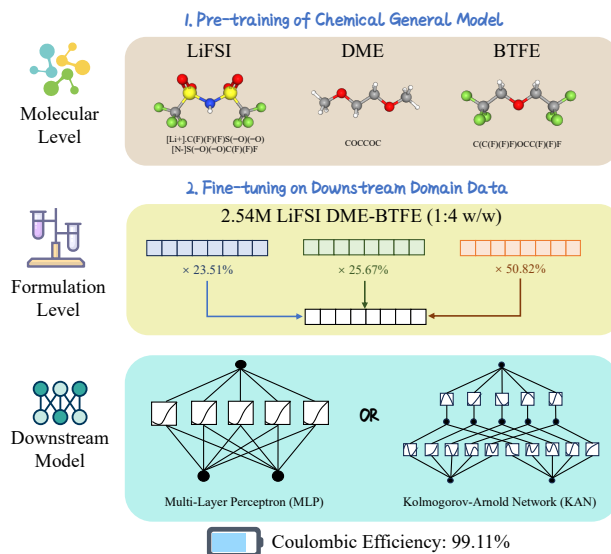


Figure 1: Overview of our method’s two-stage paradigm: pre-training a chemical general model and fine-tuning on downstream domain data.

for individual compounds but does not guide the comprehensive design of new formulations (Abolhasani and Kumacheva 2023). Fortunately, research has shown that modern energy storage devices typically use liquid electrolytes composed of one or more organic solvents and salt additives, and their formulations have a significant impact on CE (Jie et al. 2020; Yu et al. 2022). Thus, we can predict CE among a large number of electrolyte formulations and screen out those with high CE to recommend to chemical researchers, significantly reducing the workload of experimental validation.

To deal with this challenge, existing works are mainly based on two representative paradigms: machine learning (Kim et al. 2023; Narayanan Krishnamoorthy et al. 2022) and deep learning methods (Zeng et al. 2024; Soares et al. 2023; Ross et al. 2022; Sharma et al. 2023). The former approaches predict the CE of electrolytes via a supervised learning model such as regression, which takes selective features of components (e.g., redox potentials, dielec-

tric constants, ionic conductivity, and elemental composition) as input. This process requires intelligent input feature selection and reliable computational methods, which raises the critical issue of error propagation from estimating input features to model predictions (e.g., Kim et al. (2023) ignore the structural information of chemical molecules). An exemplary work in the latter approaches is MultiModal-MoLFormer (Soares et al. 2023), which leverages extensive chemical information learned from unlabeled corpora in pre-training to predict the CE of electrolytes. However, its predictive performance remains suboptimal, with a Root Mean Square Error (RMSE) of only 0.195 on the test set. Furthermore, data augmentation by shuffling the order of electrolyte components effectively increased the dataset size from 147 to 27,266 samples, yet limited diversity may lead to overfitting during training.

To address the above issues, we propose a novel electrolyte property prediction method COEFF (COLUMbic Efficiency prediction via Fine-tuned models). As illustrated in Figure 1, COEFF is intensively designed for learning the relationship between electrolyte composition and CE, which consists of two stages: pre-training of chemical general models and fine-tuning on downstream domain data. First, we adopt the publicly available MoLFormer (Ross et al. 2022), which is constructed by pre-training an efficient Transformer (Vaswani et al. 2017) encoder on a large unlabeled chemical corpus to obtain embeddings at the molecular level. The input of MoLFormer conforms to the Simplified Molecular Input Linear Entry Specification (SMILES), which can represent both the elemental composition and structural information of chemical molecules. For our application, we independently input all solvents and salts in the electrolyte into MoLFormer to extract the chemical features of each component. Then, we multiply the token embeddings of all SMILES molecules by their corresponding ratios and sum them to obtain representations at the formulation level. This is similar to concatenating all embeddings along the token length dimension, followed by a weighted average pooling layer, with the weights derived from the ratios of the electrolyte components. Finally, we feed electrolyte embeddings into a downstream model, including Multi-layer Perceptron (COEFF-MLP) or Kolmogorov–Arnold Networks (COEFF-KAN) (Liu et al. 2024b), and the output is the predicted value of CE. Our work demonstrates the potential of deep learning in electrolyte design. By harnessing the power of language models, we can accelerate the discovery and optimization of new formulations, significantly reducing the experimental validation workload for chemical researchers, and potentially revolutionizing various industries.

Experimental results on a real-world test set with 13 data points show that our method (Min. 0.132 for COEFF-MLP and Min. 0.110 for COEFF-KAN) achieves significant and consistent improvement in the RMSE metric for predicting CE compared to all baselines, including machine learning (Min. 0.170) and deep learning (Min. 0.195) methods. We will publish all source codes and datasets of this work on GitHub for further research explorations.

In summary, the main contributions of this paper are threefold: (1) We focus on the task of predicting CE based

on electrolyte components and propose a novel method COEFF, which consists of two stages: pre-training a chemical general model and fine-tuning on downstream domain data. (2) To the best of our knowledge, we are the first to introduce KAN networks into the task of electrolyte property prediction and achieve better performance than MLP. (3) We conduct extensive experiments on real-world datasets and show that COEFF outperforms previous state-of-the-art works.

Related Work

Language Models for Chemistry

In recent years, the realm of large language models has seen significant advancements, highlighting their remarkable ability to understand intricate chemical language representations (Pan 2023; Jablonka et al. 2024; Castro Nascimento and Pimentel 2023). Studies have shown that the two-stage paradigm has great potential: first pre-training on large unlabeled datasets and then fine-tuning on a specific downstream task (Schwaller et al. 2019; Ross et al. 2022; Moret et al. 2023). Leveraging self-supervised learning, these methods successfully minimize reliance on labeled data and specific tasks. While pre-trained language models perform well in predicting molecular properties (Liu et al. 2023b; Chen and Bajorath 2023), their practical implementation on further downstream tasks is still in its early stages and largely limited to sequencing problems such as predicting protein sequences (Madani et al. 2023), polymers (Chen, Tao, and Li 2021), and chemical reactions (Ranković and Schwaller 2023). Moreover, prediction errors of most methods (Soares et al. 2023; Sharma et al. 2023; Kim et al. 2023) in the electrolyte field are larger than experimental errors, making them difficult to achieve the goal of practical application. We focus on the rarely studied task of CE prediction and propose a novel method COEFF following the two-stage paradigm.

Kolmogorov–Arnold Networks

Inspired by the Kolmogorov–Arnold representation theorem (Kolmogorov 1961), researchers propose Kolmogorov–Arnold Networks (KANs) (Liu et al. 2024b) as promising alternatives to MLPs. Unlike MLPs, KANs have learnable activation functions on weights rather than fixed ones on neurons. Recent studies have shown that in some specific domains, KANs have advantages in accuracy (Seydi 2024; Bresson et al. 2024; Kiamari, Kiamari, and Krishnamachari 2024), interpretability (Li et al. 2024; Yang, Qin, and Yu 2024; Xu, Chen, and Wang 2024), continuous learning (Liu et al. 2024a), parameter efficiency (Abueidda, Pantidis, and Mobasher 2024; Cheon 2024), etc. In the field of science, PIKAN (Liu et al. 2024b; Shukla et al. 2024) combines physics-informed neural networks (Raissi, Perdikaris, and Karniadakis 2019) and KANs to solve a 2D Poisson equation, and DeepOKAN (Abueidda, Pantidis, and Mobasher 2024) uses a KAN operator network based on Gaussian radial basis functions to solve a 2D orthotropic elasticity problem. In the field of image processing, U-KAN (Li et al. 2024) redesigns the established U-Net (Ronneberger,

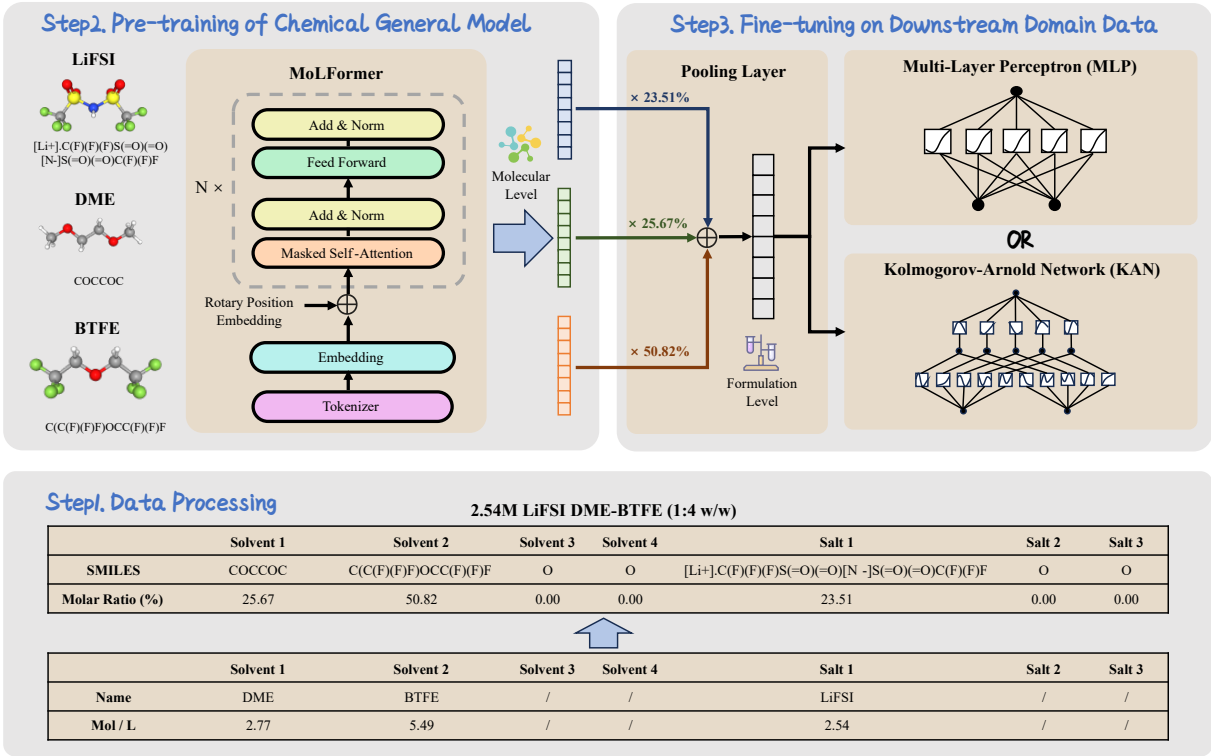


Figure 2: Overview of our proposed COEFF framework.

Fischer, and Brox 2015) pipeline for medical image segmentation by integrating the dedicated KAN layers on the tokenized intermediate representation, and KCN (Cheon 2024) introduces KANs in various pre-trained convolutional neural network models for remote sensing scene classification tasks. In the field of human-computer interaction, iKAN (Liu et al. 2024a) is an incremental learning framework for wearable sensor human activity recognition that tackles two challenges simultaneously: catastrophic forgetting and non-uniform inputs. Inspired by the above works, we apply KANs to the electrolyte field for the first time and obtain better experimental results compared with MLPs.

Methodology

Preliminary

Our task is to predict the battery’s Coulombic Efficiency through the input of electrolyte compositions. Suppose an electrolyte has n SMILES molecules $\mathcal{S} = \{s_1, s_2, \dots, s_n\}$ and corresponding molar ratios $\mathcal{P} = \{p_1, p_2, \dots, p_n\}$. Utilizing a pre-trained chemical language model, we can obtain a SMILES embedding set $\mathcal{X} = \{\mathbf{x}_1, \mathbf{x}_2, \dots, \mathbf{x}_n\}$, where each \mathbf{x}_i represents the embedding of a single SMILES molecule.

We try two different network structures for the downstream task: (1) MLP aims to replicate complex functional mappings via a series of nonlinear transformations across multiple layers. The blocks can be formally represented as:

$$\text{MLP}(\mathbf{x}) = (\mathbf{W}_{L-1} \circ \sigma \circ \mathbf{W}_{L-2} \circ \dots \circ \sigma \circ \mathbf{W}_0) \mathbf{x} \quad (1)$$

where \mathbf{W}_i denotes the weight matrix, σ denotes the activation function, and \mathbf{x} denotes the model input. (2) KAN is inspired by the Kolmogorov-Arnold representation theorem, and an L-layer KAN operates analogously to an MLP, comprising a sequence of nested KAN layers. The blocks can be formally represented as:

$$\text{KAN}(\mathbf{x}) = (\Phi_{L-1} \circ \Phi_{L-2} \circ \dots \circ \Phi_1 \circ \Phi_0) \mathbf{x} \quad (2)$$

where Φ_i denotes the function matrix corresponding to the i^{th} KAN layer. For each KAN layer with n_{in} -dimensional input and n_{out} -dimensional output, Φ can be defined as a matrix of 1D functions:

$$\Phi = \{\phi_{q,p}\} \quad p = 1, 2, \dots, n_{\text{in}}, q = 1, 2, \dots, n_{\text{out}}. \quad (3)$$

Overview of Method

Our method COEFF, illustrated in the Figure 2, is built upon an optimized MolFormer architecture, which is capable of capturing sufficiently precise chemical and structural information solely from SMILES representations.

First, we employ MolFormer, a pre-trained Transformer encoder, to generate embeddings for chemical molecules. The dataset comprises a subset from 10% of both the Zinc and PubChem datasets. We feed each SMILES, s_i , individually into MolFormer to obtain the token embeddings of all SMILES molecules \mathbf{x}_i , a vector that represents the chemical features of each component. After that, we scale \mathbf{x}_i by their corresponding molar ratios p_i and subsequently aggregate these weighted embeddings through summation to yield

a feature vector that characterizes the entire electrolyte embedding \mathbf{x} . This is similar to concatenating all embeddings along the token length dimension, followed by a weighted average pooling layer, with the weights derived from the ratios of the electrolyte components. Finally, we input the electrolyte embedding \mathbf{x} into MLP or KAN to predict the CE of electrolyte compositions.

Data Processing

The dataset (Kim et al. 2023) confines attention to solvent volume and salt molarity, emphasizing elemental composition’s role in CE. By approximating weight and volume ratios, potential discrepancies are introduced. Thus, adopting molar ratios for formulation enhances accuracy in simulating experimental scenarios.

We converted electrolyte compositions into SMILESs with accompanying molar ratios, better representing the relationship between electrolyte solvents and salts, thereby enhancing the model’s capability to predict Logarithmic Coulombic Efficiency (LCE).

Pre-training of Chemical General Model

Our approach is based on MoLFormer, an advanced transformer-based model commonly utilized for chemical language representations. MoLFormer is a large-scale masked language model that processes inputs using a series of blocks that alternate between self-attention and feed-forward connections.

MoLFormer with linear attention integrates rotary position encoding, demonstrated to outperform absolute position encoding, enhancing the representation of positional relationships in SMILES sequences without significant computational overhead. The attention mechanism is defined as follows:

$$Attention_m(Q, K, V) = \frac{\sum_{n=1}^N \langle \phi(R_m q_m), \phi(R_n q_n) \rangle v_n}{\sum_{n=1}^N \langle \phi(R_m q_m), \phi(R_n q_n) \rangle}$$

where ϕ denotes the embedding function, R the rotation matrix, and Q, K, V represent query, key, and value matrices respectively.

Using the capabilities of MoLFormer and enhancing it with the addition of relative positional embeddings, our methodology presents an advanced and efficient solution to anticipate the LCE of battery electrolytes, offering valuable insight into a variety of chemical applications.

Fine-tuning on Downstream Domain Data

We detail the SMILES’s tokenization and integration of MoLFormer-encoded SMILES with their molar ratios.

Considering that 99.4 % of the SMILES sequences comprise no more than 202 tokens, to enhance operational efficiency, we impose a limitation on sequence lengths, setting them within the range of 1 to 202 tokens.

Concatenate Input Disentangle Output (CIDO)

MultiModal-MoLFormer is splicing SMILES through `<sep>` as input to MoLFormer, which is against the format of MoLFormer pre-training, so we innovate by preprocessing: concatenating tokenised SMILES sequences before

input and later disentangling post-encoding. After encoding, the representation of each molecule is a shape tensor $B \times L \times H$, where B is the batch size, L the token count per molecule, and H denotes the embedding dimensionality. This approach capitalises on MoLFormer’s design while maintaining the integrity of distinct molecules. design while maintaining the integrity of distinct molecular profiles.

We use two methods: COEFF-MLP and COEFF-KAN as our downstream network structure to predict the CE of the electrolyte formulation. This configuration processes the electrolyte embedding, \mathbf{x} , to make the prediction, thereby leveraging the model’s capacity to capture intricate relationships within the molecular structures for enhanced efficiency forecasts. The number of layers in the two methods is not fixed. Here we represent the representation obtained by \mathbf{x} after the i -th layer

$$\mathbf{x}_{i+1} = \text{MLP}_i(\mathbf{x}_i). \quad (4)$$

$$\mathbf{x}_{i+1} = \text{KAN}_i(W_i \times \mathbf{x}_i \mid \Phi_i). \quad (5)$$

Experiments

Experimental Setup

Datasets To validate the efficacy of our method, we apply it to the Li/Cu half-cell-based dataset (Kim et al. 2023), collected from some chemical literature. Electrolyte formulations in this dataset consist of 2 to 7 components each, described by SMILES. To numerically amplify the change in output with respect to electrolyte variation, CE is converted to a logarithmic format (LCE, defined as $-\log(1 - \text{CE})$). We remove an entry with a repeated ratio but different measurement methods, and correct errors in some ratios and molecular information. Thus, we obtain 149 electrolyte formulations for training and 13 entries as a test set \mathcal{T}_{out} . Additionally, we split the 149 data into training and test sets in a ratio of 7:3 to obtain \mathcal{T}_{in} . Box plots illustrated in Figure 3 provide a clear visualization of the distribution of LCE outputs for the training data based on the count of formulation constituents.

Baselines We compare our method with some strong baselines, which are divided into two groups: machine learning (†) and deep learning (‡) approaches.

- **Kim et al.** (†) (Kim et al. 2023) use the elemental composition of electrolytes as input features for the machine learning models (e.g., linear regression, random forest, boosting, and bagging) to predict CE.
- **F-GCN** (‡) (Sharma et al. 2023) assembles multiple Graph Convolution Networks (GCNs) in parallel to intuitively represent formulation constituents, including no-TL F-GCN and TL F-GCN.
- **MoLFormer** (‡) (Ross et al. 2022) trains an efficient Transformer encoder on SMILES sequences of 1.1 billion unlabeled molecules, using a linear attention mechanism and rotational position embedding.
- **MultiModal-MoLFormer** (‡) (Soares et al. 2023) utilizes extensive chemical information learned in pre-training to predict the performance of electrolytes, allowing multiple molecules in SMILES format as input.

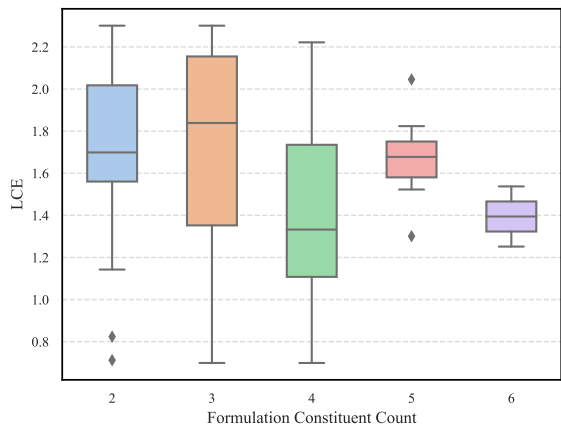


Figure 3: Box plots depict the distribution of LCE outputs for training data based on the formulation constituent count. The outer whiskers represent the minimum and maximum values, the central line represents the median, and the colored box represents the 25th to 75th percentile of the data. Data points outside the outer whiskers are outliers observed in the data.

- **BART-SA** (‡) (Priyadarsini et al. 2024) obtains molecular representations of individual electrolyte components from the pre-trained BART model, then scales and sums to form a unified feature vector.
- **Uni-ELF** (‡) (Zeng et al. 2024) is a multi-level representation learning framework that enhances electrolyte design through two-stage pre-training.

Metrics We use Root Mean Square Error (RMSE) as the metric that can be calculated by the following formula:

$$\text{RMSE} = \sqrt{\frac{1}{N} \sum_{i=1}^N (y_i - \hat{y}_i)^2} \quad (6)$$

where N is the number of samples, y_i and \hat{y}_i are the experimentally observed and model-predicted LCEs, respectively.

Hyperparameters and Training Details For COEFF-MLP, we set the dimensions of MoLFormer embedding to 768, headers of attention layers to 12, and the number of encoder layers to 12. The downstream MLP consists of 2 linear layers with dropout 0.2 and ReLU (Agarap 2019) activation functions. We optimize the parameters with AdamW (Loshchilov and Hutter 2019) with batch size 4, learning rate 5×10^{-5} , and epochs 100. For COEFF-KAN, we set 2 KANs and a linear layer in the downstream network, while other hyperparameters are consistent with COEFF-MLP.

Main Experimental Results

We conduct comparative experiments to evaluate the effectiveness of each method in the predicting LCE task. Table 1 shows the RMSE results of all models on \mathcal{T}_{in} and \mathcal{T}_{out} test sets.

Table 1: RMSE results of LCE prediction for different methods, where bold indicates the best performance and underline denotes the second-best performance. * stands for the ratio of training set to test set is 8:2, so it is not included in the comparison.

Methods	LCE	
	\mathcal{T}_{in}	\mathcal{T}_{out}
Linear Regression	0.585	0.170
Random Forest	0.577	-
Boosting	0.587	-
Bagging	0.583	-
no-TL F-GCN	-	0.779
TL F-GCN	-	0.390
MoLFormer	-	0.213
MultiModal-MoLFormer	-	0.195
BART-SA*	0.148	-
Uni-ELF	0.184	-
COEFF-MLP	0.221	<u>0.132</u>
COEFF-KAN	<u>0.186</u>	0.110

First, we observe that our method outperforms machine learning models on all datasets. Especially on \mathcal{T}_{in} , the RMSE of COEFF-KAN is 0.399, 0.391, 0.401, and 0.397 lower than linear regression, random forest, boosting, and bagging respectively. The performance of these approaches is limited by whether the feature selection is appropriate and complete. For example, Kim et al. (2023) use the elemental composition of liquid electrolytes as input features. They successfully reveal that a reduction in the solvent oxygen content is critical for superior CE but overlook structural information of chemical molecules (e.g., geometric arrangements of elements in isomers). This subtle distinction has been shown to affect electrolyte properties and battery performance (Zhang and Viswanathan 2020, 2021).

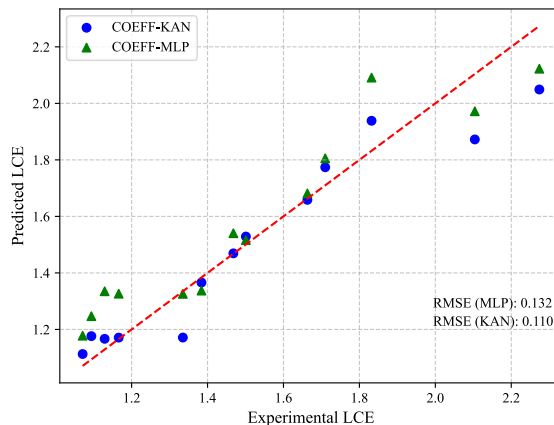


Figure 4: Parity plots show predicted LCE values as scatter-plots with respect to the actual values.

Second, it is noticed that our method achieves state-of-the-art performance among all deep learning models on

\mathcal{T}_{out} . In particular, the RMSE of COEFF-KAN is 0.280, 0.103, and 0.085 lower than F-GCN, MoLFormer, and MultiModal-MoLFormer. Although our method, like most others, follows a two-stage paradigm, it benefits from the accurate representation of chemical molecules by MoLFormer, weighted average pooling at the formulation level, and performance advantages of KANs in the scientific domain. Additionally, unlike MultiModal-MoLFormer, which uses data augmentation to expand the training set to 27,266, our model only requires fine-tuning with just over a hundred samples to achieve more accurate predictions.

Third, experimental results demonstrate that introducing KANs into downstream networks can better predict the LCE of electrolytes. Specifically, the RMSE of COEFF-KAN is 0.030 and 0.022 lower than that of COEFF-MLP on \mathcal{T}_{in} and \mathcal{T}_{out} , respectively. We speculate that there are two main reasons: (1) Better interpretability: Compared to MLPs, design of KANs network structure makes the model’s behavior easier to understand. By observing the external connection patterns, we can have an insight into interactions between input features. The internal activation functions help visualize how a single variable affects the output, thereby increasing the transparency of models. (2) More efficient learning with limited data size: Theoretically, KANs can achieve better fitting effects with fewer samples, because they learn more complex and generalizable function mappings through the synergy of trainable network structures and activation functions.

Finally, our method is stable and effective for predicting LCE against unseen data. As shown in Figure 4, most of the predicted data points for COEFF-MLP and COEFF-KAN are close to the perfect prediction line and have similar distributions. The generalization can make COEFF adapt to practical application scenarios and help chemical researchers reduce the workload of experimental verification.

Ablation Experiments

In this section we will perform ablation experiments and analyses in terms of CIDO and KAN respectively

CIDO. Table 2 reports the ablation with or without the method. In the LCE prediction task, MLP and KAN use the CIDO method to improve performance on \mathcal{T}_{out} by 0.261 and 0.278, respectively. The results show that using CIDO can be effective for model prediction while saving some training time overhead with the same machine and configuration.

Methods	\mathcal{T}_{out}	Time(s)
COEFF-MLP w/o CIDO	0.393	715
COEFF-MLP w/ CIDO	0.132	705
COEFF-KAN w/o CIDO	0.388	741
COEFF-KAN w/ CIDO	0.110	725

Table 2: RMSE results of LCE prediction at w/ and w/o CIDO method.

KAN. We used MLP with different depths and widths as a baseline to compare with KAN. Both MLP and KAN were trained with 100 epochs using CIDO, and the RMSE of the

lowest-loss epoch of the validation set on the test set is plotted as Figure 5. As can be seen from the figure, testing on the \mathcal{T}_{out} , we find that the optimal value of KAN is 17.42% better than that of MLP, thus proving the effectiveness of the downstream network using KAN. At the same time, we find that the results of KAN with different widths tend to stabilize with the network depth RMSE, but MLP performs better at 2-3 layers of the network architecture, and the performance is gradually unstable as the depth of the network deepens.

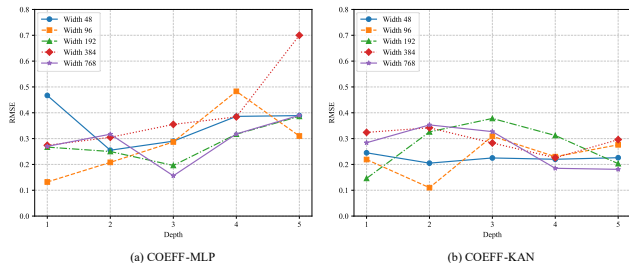


Figure 5: RMSE results of LCE prediction at different network depths and widths.

Conclusion and Future Work

In this paper, we propose a novel method COEFF for accurately predicting the LCE of electrolytes. There are two main contributions:

- (1) We adopt a two-stage paradigm: pre-training a chemical general model and fine-tuning it on domain data.
- (2) We innovatively replace the downstream MLPs with KANs.

In the experiments, we show that our method significantly and consistently outperforms state-of-the-art models on a real-world test set \mathcal{T}_{out} .

In the future, we will explore the following directions:

- (1) We will apply our model to more electrolyte properties (e.g., charge/discharge current and battery cycle life), more chemical fields, and even material science subfields, as the two-stage paradigm is universal.
- (2) We will fully utilize the interpretability of KANs to find the quantitative relationship between electrolyte formulations and CE through function fitting and visualization.

References

- Abolhasani, M.; and Kumacheva, E. 2023. The rise of self-driving labs in chemical and materials sciences. *Nature Synthesis*, 2(6): 483–492.
- Abueidda, D. W.; Pantidis, P.; and Mobasher, M. E. 2024. DeepOKAN: Deep Operator Network Based on Kolmogorov Arnold Networks for Mechanics Problems. arXiv:2405.19143.
- Agarap, A. F. 2019. Deep Learning using Rectified Linear Units (ReLU). arXiv:1803.08375.
- Agre, P.; Molina, M.; and Chu, S. 2017. The real climate debate. *Nature*, 550(7675): S62–S64.

- Aykol, M.; Herring, P.; and Anapolsky, A. 2020. Machine learning for continuous innovation in battery technologies. *Nature Reviews Materials*, 5(10): 725–727.
- Bresson, R.; Nikolentzos, G.; Panagopoulos, G.; Chatzianastasis, M.; Pang, J.; and Vazirgiannis, M. 2024. KAGNNs: Kolmogorov-Arnold Networks meet Graph Learning. arXiv:2406.18380.
- Castro Nascimento, C. M.; and Pimentel, A. S. 2023. Do large language models understand chemistry? a conversation with chatgpt. *Journal of Chemical Information and Modeling*, 63(6): 1649–1655.
- Chen, G.; Tao, L.; and Li, Y. 2021. Predicting polymers' glass transition temperature by a chemical language processing model. *Polymers*, 13(11): 1898.
- Chen, H.; and Bajorath, J. 2023. Designing highly potent compounds using a chemical language model. *Scientific Reports*, 13(1): 7412.
- Cheon, M. 2024. Kolmogorov-Arnold Network for Satellite Image Classification in Remote Sensing. arXiv:2406.00600.
- Jablonka, K. M.; Schwaller, P.; Ortega-Guerrero, A.; and Smit, B. 2024. Leveraging large language models for predictive chemistry. *Nature Machine Intelligence*, 6(2): 161–169.
- Jie, Y.; Ren, X.; Cao, R.; Cai, W.; and Jiao, S. 2020. Advanced liquid electrolytes for rechargeable Li metal batteries. *Advanced Functional Materials*, 30(25): 1910777.
- Kiamari, M.; Kiamari, M.; and Krishnamachari, B. 2024. GKAN: Graph Kolmogorov-Arnold Networks. arXiv:2406.06470.
- Kim, S. C.; Oyakhire, S. T.; Athanitis, C.; Wang, J.; Zhang, Z.; Zhang, W.; Boyle, D. T.; Kim, M. S.; Yu, Z.; Gao, X.; et al. 2023. Data-driven electrolyte design for lithium metal anodes. *Proceedings of the National Academy of Sciences*, 120(10): e2214357120.
- Kolmogorov, A. N. 1961. *On the representation of continuous functions of several variables by superpositions of continuous functions of a smaller number of variables*. American Mathematical Society.
- Li, C.; Liu, X.; Li, W.; Wang, C.; Liu, H.; and Yuan, Y. 2024. U-KAN Makes Strong Backbone for Medical Image Segmentation and Generation. arXiv:2406.02918.
- Liu, J.; Zhang, Y.; Zhou, J.; Wang, Z.; Zhu, P.; Cao, Y.; Zheng, Y.; Zhou, X.; Yan, C.; and Qian, T. 2023a. Advances and prospects in improving the utilization efficiency of lithium for high energy density lithium batteries. *Advanced Functional Materials*, 33(34): 2302055.
- Liu, M.; Bian, S.; Zhou, B.; and Lukowicz, P. 2024a. iKAN: Global Incremental Learning with KAN for Human Activity Recognition Across Heterogeneous Datasets. arXiv:2406.01646.
- Liu, Y.; Zhang, R.; Li, T.; Jiang, J.; Ma, J.; and Wang, P. 2023b. MolRoPE-BERT: An enhanced molecular representation with Rotary Position Embedding for molecular property prediction. *Journal of Molecular Graphics and Modeling*, 118: 108344.
- Liu, Z.; Wang, Y.; Vaidya, S.; Ruehle, F.; Halverson, J.; Soljačić, M.; Hou, T. Y.; and Tegmark, M. 2024b. KAN: Kolmogorov-Arnold Networks. arXiv:2404.19756.
- Loshchilov, I.; and Hutter, F. 2019. Decoupled Weight Decay Regularization. arXiv:1711.05101.
- Madani, A.; Krause, B.; Greene, E. R.; Subramanian, S.; Mohr, B. P.; Holton, J. M.; Olmos, J. L.; Xiong, C.; Sun, Z. Z.; Socher, R.; et al. 2023. Large language models generate functional protein sequences across diverse families. *Nature Biotechnology*, 41(8): 1099–1106.
- Moret, M.; Pachon Angona, I.; Cotos, L.; Yan, S.; Atz, K.; Brunner, C.; Baumgartner, M.; Grisoni, F.; and Schneider, G. 2023. Leveraging molecular structure and bioactivity with chemical language models for de novo drug design. *Nature Communications*, 14(1): 114.
- Narayanan Krishnamoorthy, A.; Wölke, C.; Diddens, D.; Maiti, M.; Mabrouk, Y.; Yan, P.; Grünebaum, M.; Winter, M.; Heuer, A.; and Cekic-Laskovic, I. 2022. Data-Driven Analysis of High-Throughput Experiments on Liquid Battery Electrolyte Formulations: Unraveling the Impact of Composition on Conductivity. *Chemistry-Methods*, 2(9): e202200008.
- Pan, J. 2023. Large language model for molecular chemistry. *Nature Computational Science*, 3(1): 5–5.
- Priyadarsini, I.; Sharma, V.; Takeda, S.; Kishimoto, A.; Hamada, L.; and Shinohara, H. 2024. Improving Performance Prediction of Electrolyte Formulations with Transformer-based Molecular Representation Model. arXiv:2406.19792.
- Raissi, M.; Perdikaris, P.; and Karniadakis, G. E. 2019. Physics-informed neural networks: A deep learning framework for solving forward and inverse problems involving nonlinear partial differential equations. *Journal of Computational physics*, 378: 686–707.
- Ranković, B.; and Schwaller, P. 2023. BoChemian: Large language model embeddings for Bayesian optimization of chemical reactions. In *NeurIPS*.
- Ronneberger, O.; Fischer, P.; and Brox, T. 2015. U-net: Convolutional networks for biomedical image segmentation. In *MICCAI*.
- Ross, J.; Belgodere, B.; Chenthamarakshan, V.; Padhi, I.; Mroueh, Y.; and Das, P. 2022. Large-scale chemical language representations capture molecular structure and properties. *Nature Machine Intelligence*, 4(12): 1256–1264.
- Schwaller, P.; Laino, T.; Gaudin, T.; Bolgar, P.; Hunter, C. A.; Bekas, C.; and Lee, A. A. 2019. Molecular transformer: a model for uncertainty-calibrated chemical reaction prediction. *ACS central science*, 5(9): 1572–1583.
- Seydi, S. T. 2024. Unveiling the Power of Wavelets: A Wavelet-based Kolmogorov-Arnold Network for Hyperspectral Image Classification. arXiv:2406.07869.
- Sharma, V.; Giammona, M.; Zubarev, D.; Tek, A.; Nugyuen, K.; Sundberg, L.; Congiu, D.; and La, Y.-H. 2023. Formulation graphs for mapping structure-composition of battery electrolytes to device performance. *Journal of Chemical Information and Modeling*, 63(22): 6998–7010.

Shukla, K.; Toscano, J. D.; Wang, Z.; Zou, Z.; and Karniadakis, G. E. 2024. A comprehensive and FAIR comparison between MLP and KAN representations for differential equations and operator networks. *arXiv:2406.02917*.

Soares, E.; Sharma, V.; Brazil, E. V.; Cerqueira, R.; and Na, Y.-H. 2023. Capturing Formulation Design of Battery Electrolytes with Chemical Large Language Model. In *NeurIPS*.

Tian, Y.; Zeng, G.; Rutt, A.; Shi, T.; Kim, H.; Wang, J.; Koettgen, J.; Sun, Y.; Ouyang, B.; Chen, T.; et al. 2020. Promises and challenges of next-generation “beyond L-ion” batteries for electric vehicles and grid decarbonization. *Chemical reviews*, 121(3): 1623–1669.

Vaswani, A.; Shazeer, N.; Parmar, N.; Uszkoreit, J.; Jones, L.; Gomez, A. N.; Kaiser, Ł.; and Polosukhin, I. 2017. Attention is all you need. In *NeurIPS*.

Xu, K.; Chen, L.; and Wang, S. 2024. Kolmogorov-Arnold Networks for Time Series: Bridging Predictive Power and Interpretability. *arXiv:2406.02496*.

Yang, S.; Qin, L.; and Yu, X. 2024. Endowing Interpretability for Neural Cognitive Diagnosis by Efficient Kolmogorov-Arnold Networks. *arXiv:2405.14399*.

Yu, Z.; Rudnicki, P. E.; Zhang, Z.; Huang, Z.; Celik, H.; Oyakhire, S. T.; Chen, Y.; Kong, X.; Kim, S. C.; Xiao, X.; et al. 2022. Rational solvent molecule tuning for high-performance lithium metal battery electrolytes. *Nature Energy*, 7(1): 94–106.

Yuan, S.; Kong, T.; Zhang, Y.; Dong, P.; Zhang, Y.; Dong, X.; Wang, Y.; and Xia, Y. 2021. Advanced electrolyte design for high-energy-density Li-metal batteries under practical conditions. *Angewandte Chemie*, 133(49): 25828–25842.

Zeng, B.; Chen, S.; Liu, X.; Chen, C.; Deng, B.; Wang, X.; Gao, Z.; Zhang, Y.; E, W.; and Zhang, L. 2024. Uni-ELF: A Multi-Level Representation Learning Framework for Electrolyte Formulation Design. *arXiv:2407.06152*.

Zhang, Y.; and Viswanathan, V. 2020. Not All fluorination is the same: Unique effects of fluorine functionalization of ethylene carbonate for tuning solid-electrolyte interphase in Li metal Batteries. *Langmuir*, 36(39): 11450–11466.

Zhang, Y.; and Viswanathan, V. 2021. Design rules for selecting fluorinated linear organic solvents for li metal batteries. *The Journal of Physical Chemistry Letters*, 12(24): 5821–5828.